

Inclination Effects on Circumferential Film Flow Distribution in Annular Gas/Liquid Flows

G. Geraci and B. J. Azzopardi

School of Chemical, Environmental and Mining Engineering, University of Nottingham,
University Park, Nottingham, NG7 2RD, U.K.

H.R.E. van Maanen

Shell Global Solution International, Upstream Sector, Advanced Production Management Team,
P.O. Box 60, 2280 AB Rijswijk, Netherlands

DOI 10.1002/aic.11155

Published online March 28, 2007 in Wiley InterScience (www.interscience.wiley.com).

Measurements of the circumferentially resolved axial liquid film flow rate have been obtained for a 38 mm internal dia. pipe at inclinations of 0°, 20°, 45°, 70 and 85° from the horizontal. The method employed is based on that used by Butterworth, and consists of a film extraction technique which utilizes a unit with a wall that is porous over a sector of the pipe. Liquid entrained fraction was determined from the total film flow rate. Results show that the local liquid film flow rate is not symmetrical. Flow rates are higher on the lower part of the pipe. As the inclination angle deviates from horizontal, the film flow rate becomes systematically less asymmetric. There is not a strong dependence of the entrained fraction on pipe inclination. For the case when the pipe is horizontal, the circumferential variation of film flow rate is well predicted by a horizontal annular flow model. © 2007 American Institute of Chemical Engineers AIChE J, 53: 1144–1150, 2007

Keywords: gas-liquid flow, annular flow, film flow rate, entrained fraction, pipe inclination

Introduction

Gas-liquid flow occurs widely in the power generation and hydrocarbon production industries. When a gas-liquid mixture flows in a pipe, it has been observed that the interface between the two phases can have different characteristics depending on variables, such as inlet flow rates, fluid properties, pipe geometry and orientation of the flow. The various configurations of interfacial distributions can be classified into flow patterns. Annular flow is one of the most common flow patterns encountered in natural gas well-bores and pipelines. It occurs at high-gas and low to medium liquid flow rates, and at all pipe orientations. In this configuration, some of the liquid travels as a film on the channel walls, and the remainder is carried as drops

by the gas in the center of the channel. The fraction of liquid travelling as drops can vary from zero to close to one. The interface between the gas core and the liquid film is usually very wavy, and entrainment and deposition of liquid droplets occur through this interface.

The majority of pipes are mounted vertically or horizontally. In some cases, such as oil/gas wells where deviated drilling has been employed or risers from the sea bed to floating production facilities, the pipes are inclined at angle between the vertical and horizontal. Here, it is important to know the distribution of liquid about the pipe cross-section so as to protect adequately against erosion and corrosion. Although there have been studies of flow patterns, pressure drop and void fraction for gas/liquid flow up inclined pipes, there have been few studies which have provided more detailed information. Azzopardi and Zaidi¹ applied a laser diffraction technique to measure drop size distributions in inclined annular flow. The work was extended² to determine drop concentrations, and, hence, entrained liquid flow rates. Both measurements were averages

Current address of G. Geraci: Dept. of Petroleum Engineering, University of Tulsa, Keplinger Hall, Room #L101, Tulsa, OK 74104.

Correspondence concerning this article should be addressed to B. J. Azzopardi at barry.azzopardi@nottingham.ac.uk.

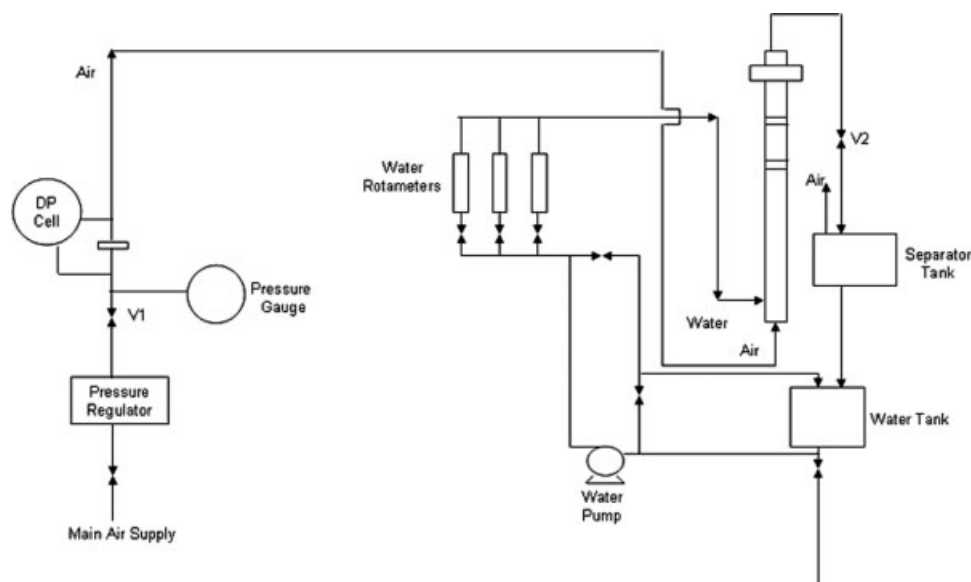


Figure 1. Arrangement of the inclinable flow facility.

across a diameter. There have been two studies which provide circumferential film thickness measurements.^{3,4} These show much thicker films at the bottom than at the top of the pipe. Circumferentially resolved film flow rate measurements have been obtained for annular flow in horizontal pipes.^{5,6} These again show large differences between top and bottom. However, hitherto there have been no data on the circumferential film flow variation for annular flow in inclined pipes.

There are a number of sources which provide values of the fraction of entrained liquid in horizontal annular flow.^{7–12}

There are no models currently available for annular flow in inclined pipes. There have been a number of models published for horizontal annular flow. All allow for drainage of the liquid around the sides of the pipe driving by gravity. They invoke different mechanisms for the replenishment/retention of liquid at the top and sides of the pipe. These include: entrainment from the bottom and depletion onto the top; secondary flow in the gas, caused by rougher film on the bottom than at the top, providing an upward shear on the film; pumping action through the waves on the film interface. Azzopardi¹³ has examined these models, and has shown that they all give good predictions of circumferentially varying properties, such as film flow rate and film thickness.

Experimental Arrangements

Flow facility

The annular two-phase flow experiments were carried out on an inclinable rig in the Chemical Engineering Laboratory of the School of Chemical, Environmental and Mining Engineering, University of Nottingham. The arrangement is shown in Figure 1. The 38 mm internal dia. pipe was mounted on an inclinable beam so that it could be positioned at any angle between vertical and horizontal. The distance between the injection point, where the liquid is introduced as a film, and the test section was 132 pipe dia. Therefore, fairly well developed annular flow was anticipated. The experiments reported here

concentrated on a small range of gas mass flow rates, motivated by interest in wet-gas metering of which this project was a part. Gas mass flow rates of 0.03 and 0.04 kg/s were examined which correspond to gas superficial velocities of 15 and 21.5 m/s. The liquid flow rates considered were 0.0079 and 0.0131 kg/s, which correspond to liquid superficial velocities of 0.007 and 0.011 m/s. The pressure in the test section ranged from 1.3 to 1.5 bars absolute. Air was supplied from the laboratory compressed air mains, and its flow rate was measured by an orifice plate and controlled by valve V1, Figure 1. Water was pumped from a 300 L supply tank and its flow was metered by one of the three calibrated rotameters. After passing down the length of the inclinable beam, the water entered into the main pipe through a porous wall section located 0.5 m from the start of it. Valve V2 on the two-phase exit line upstream of a disengagement tank allowed a constant pressure to be set at the end of the pipe. The air/water mixture was separated in a large vessel. Air was released to the atmosphere and water was returned to the supply tank.

Measurement method

The film extraction technique employed to determine the liquid film flow rate was similar to that used by Butterworth⁵ and Butterworth and Pulling.⁶ The basic concept was to allow a partial section of the liquid film and an amount of gas to be drawn off from the pipe into a phase separator. The liquid rate was determined by timing the flow. A partial liquid take off device was built in brass and equipped with a porous sintered wall over a limited sector of the pipe wall. The unit is shown in Figures 2 and 3 and was made of two components. The first was an external cylinder with an exit for the fluids extracted. The second was an internal cylinder equipped with a porous wall over a limited sector. This latter cylinder had an internal dia. of 38 mm. There were two 9.5 mm high fins positioned along the two sides of the porous wall section to prevent liquid being sucked in from beyond the sector. The internal cylinder containing the fins was arranged so that it could be rotated

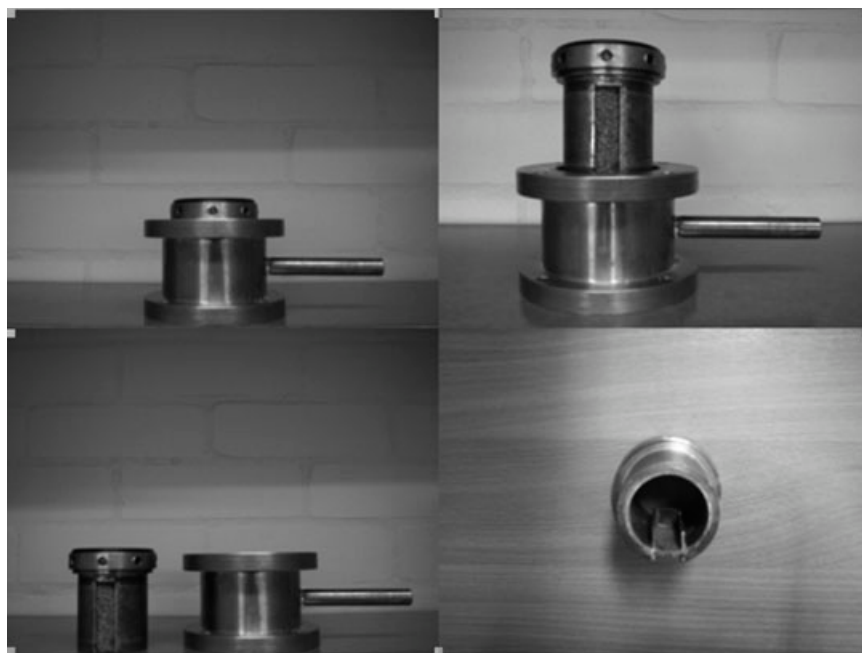


Figure 2. Partial take-off device for the pipe.

without rotating the rest of the unit. Leakages were prevented by appropriately placed O-ring seals. The fluids taken off was led by flexible tubing via a control valve to a small cyclone separator.

During the measurements, it was essential to ensure that all the liquid in the film was taken out through the porous wall. To do this, the fins were dimensioned to be just higher than the tallest waves expected. A compromise was reached between the height of the films and the highest flow rate studied.

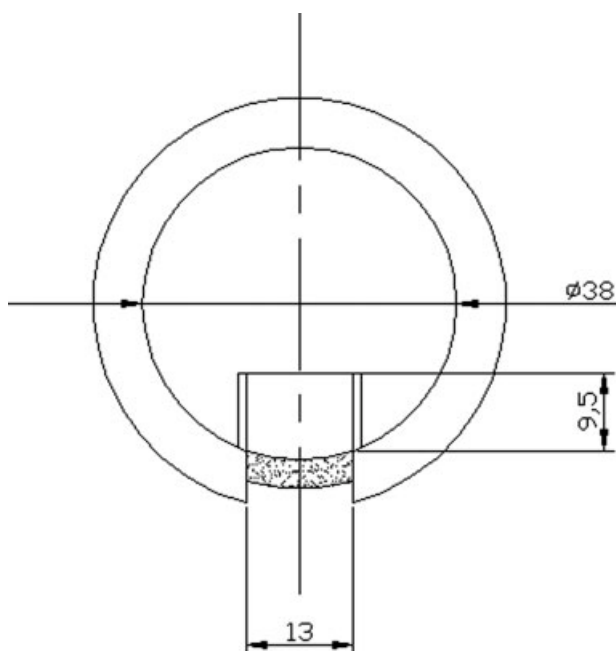


Figure 3. Internal cylinder used for the pipe.

Unit in mm.

To check the symmetry about the vertical plane, both sides of the section were studied and one side was distinguished from the other by positive and negative values of the angle, θ . Zero is at the bottom of the pipe. The unit was operated at eight different positions of the porous wall around the circumference identified in Table 1. At each flow condition and position, the air and water taken off through the porous wall were separated and their flow rates metered for a number of settings of the take-off control valve. The gas flow was metered using a rotameter while the liquid flow rate was determined by timing the discharge of known volumes of liquid. In the original work using this type of device, Butterworth and Pulling⁶ showed that straight lines could be fitted to the data and used to determine the intercept value. Extrapolation to zero gas take off gives a value of liquid flow rate which can be assumed to be the film flow over the perimeter between the fins. As with Butterworth and Pulling, it is argued here is that, at this intercept, where there is no air removed, and, hence, neither the droplet flow nor the film flow elsewhere can be dragged out by the air. With the earlier assumption, the local film flow rate per unit width of surface is given by

$$\Gamma = \omega_l / b \quad (1)$$

Table 1. Positions of the Porous Sintered Wall Unit Window

Position	Angular Position, θ (Deg)
1	-77
2	-122
3	-167
4	148
5	103
6	58
7	13
8	-32

where ω_l is the rate of the liquid film taken off at the intercept, and b is the perimeter between the fins. The value of Γ was calculated for eight positions of the porous wall sector. As the circumferential width of the sector was equal to $1/8^{\text{th}}$ of the pipe perimeter, the film flow rate, \dot{M}_{LF} , was obtained by summing the eight measurements

$$\dot{M}_{LF} = \sum_{x=1}^8 \Gamma \cdot b \quad (2)$$

Once the total liquid take off is known, the entrained fraction E can be calculated from Eq. 3

$$E = \frac{\dot{M}_L - \dot{M}_{LF}}{\dot{M}_L} = \frac{\dot{M}_{LE}}{\dot{M}_L} \quad (3)$$

where \dot{M}_L is the total liquid flow rate, and \dot{M}_{LE} is the flow rate of liquid travelling as drops.

Results and Discussion

Film flow rates were measured at inclinations of 0° , 20° , 45° , 70° and 85° from horizontal with gas and liquid mass flow rates as listed in Table 2.

In all cases studied the flow pattern observed was annular. At the lowest gas and liquid flow rates examined in the horizontal case, the film thickness on the top part of the pipe was very thin. These observations have been compared with the prediction of published models. For the horizontal case, the data are plotted on the flow pattern map of Taitel and Dukler,¹⁴ Figure 4. This shows that the two points at the lowest gas mass flow rate are expected to be in the wavy stratified flow region. However, the measurements showed that there was a film on the top of the pipe even at the lowest gas and liquid flow rates. The axes in Figure 4 are a gas Froude number and the Lockhart-Martinelli parameter. These are defined by

$$Fr = \sqrt{\frac{u_{gs}^2 \rho_g}{g D_t (\rho_l - \rho_g)}} \quad (4)$$

$$X = \frac{u_{ls}}{u_{gs}} \sqrt{\frac{\rho_l f_l}{\rho_g f_g}} \quad (5)$$

where u_{gs} and u_{ls} are the superficial velocities of the gas and liquid, ρ_g , ρ_l are the gas and liquid densities, g is the gravitational acceleration, D_t is the pipe diameter, and f_g , f_l are the friction factors, based on superficial velocities and pipe diameter. For the equivalent vertical case, the transitions to annular flow suggested^{15,16} have been considered. Taitel et al.¹⁴ proposed a critical Kutateladze number given by Eq. 6. This

Table 2. Mass Flow Rates and Superficial Velocities Employed

Gas mass Flow Rate (kg/s)	Gas Superficial Velocity (m/s)
0.03	15
0.04	21.5
Liquid mass flow rate (kg/s):	Liquid superficial velocity (m/s)
0.0079	0.007
0.0131	0.011

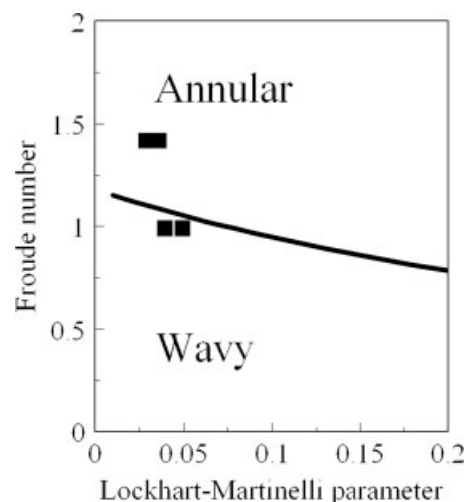


Figure 4. Conditions studied plotted on the flow pattern map of Taitel and Dukler.¹⁴

indicated a superficial gas velocities of 12.6 m/s at the transition between churn and annular flow

$$Ku = \frac{u_{gs} \sqrt{\rho_g}}{([\rho_l - \rho_g] g \sigma)^{1/4}} = 3.1 \quad (6)$$

where σ is the surface tension. In contrast, McQuillan and Whalley¹⁶ used a criterion of the dimensionless gas velocity, $u_g^* = 1$. This parameter is exactly equal to the Froude number defined in Eq. 4. From this, it was determined that the transition superficial gas velocity was 14.7 m/s. Therefore, for these experiments the flow might be expected to be annular bordering on churn.

Figures 5 to 8 show the variation of the axial film flow rate with the inclination from horizontal. The abscissa refers to the angular position of the center of the sector while the ordinate refers to the partial liquid film mass flow rate divided by the

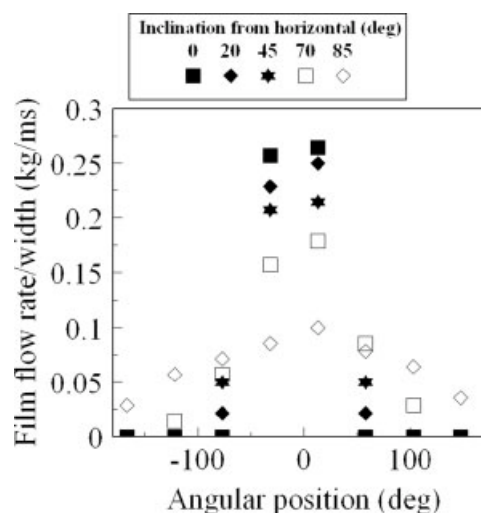


Figure 5. Liquid flow rate variation with the angle of inclination from the horizontal.

Gas superficial velocity = 21.5 m/s, liquid superficial velocity = 0.007 m/s.

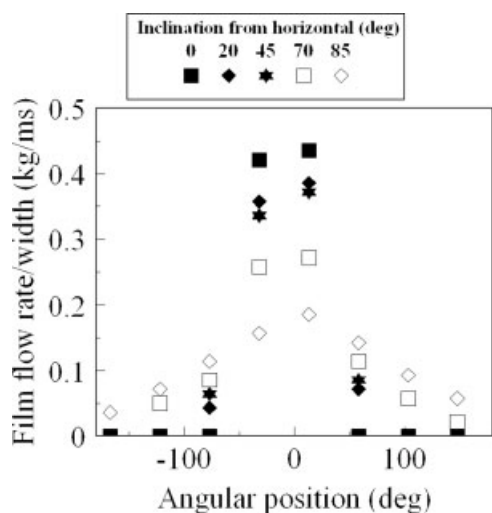


Figure 6. Liquid flow rate variation with the angle of inclination from the horizontal.

Gas superficial velocity = 21.5 m/s, liquid superficial velocity = 0.011 m/s.

width of the window given in Eq. 1. The axial film flow rate plotted is not the true local value, but an average over perimeter b . The figures show that profile of is asymmetric with higher flow rates at the bottom of the pipe. They also show that the profile becomes less asymmetric with increasing inclination from horizontal. For the horizontal case, the liquid is almost entirely present around the bottom side of the pipe. On the upper side of the pipe, the flow rate is very close to zero with a vestige of film present. For higher inclinations, the liquid spreads out and there are finite film flow rates on the upper part of the pipe. Examination of the data presented in these figures shows that there is very little effect of the gas flow rate on the film flow rate over the small range of gas flows examined. A larger effect might be expected at higher gas flow rates.

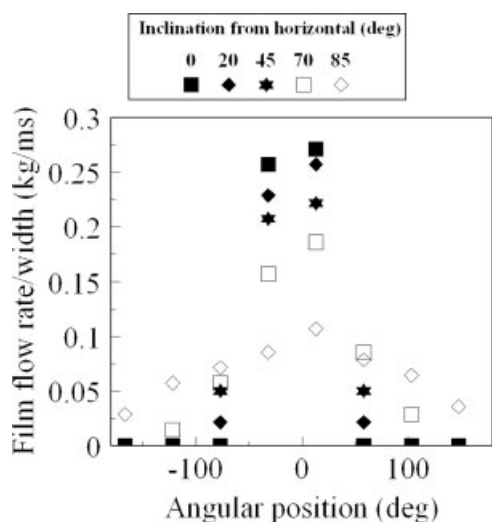


Figure 7. Liquid flow rate variation with the angle of inclination from the horizontal.

Superficial-gas velocity = 15 m/s, liquid superficial velocity = 0.007 m/s.

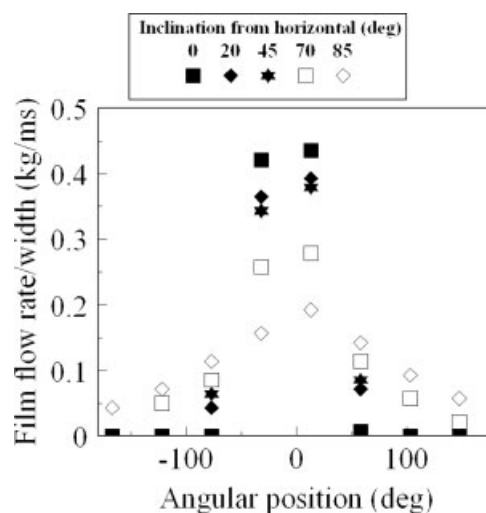


Figure 8. Liquid flow rate variation with the angle of inclination from horizontal.

Superficial gas velocity = 15 m/s, liquid superficial velocity = 0.011 m/s.

Figure 9 shows the variation of the entrained fraction with the angle of inclination. It is evident that, at the liquid flow rates studied, the orientation of the pipe has only a small effect on the liquid entrainment with a small decrease as the inclination increases except at angles very close to the vertical. To understand the reasons for this, it is essential to examine the process of drop creation. In annular flow, the majority of drops are created from the wall film by the action of gas flowing over it. However, drops are not created from the entire film interface, but very specifically they arise from disturbance waves. The most conclusive proof that waves are the source of drops was provided by Azzopardi and Whalley.¹⁷ By injecting small

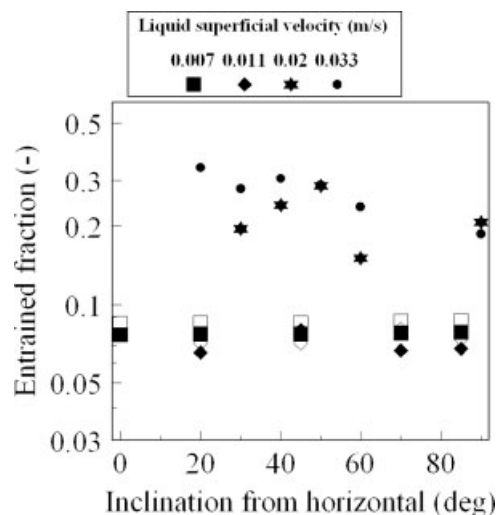


Figure 9. Entrained fraction variation with angle of inclination from horizontal and gas mass flow rate in the main section.

Open symbols: Superficial-gas velocity = 21.5 m/s; closed symbol: gas superficial velocity = 15 m/s. Data indicated by \bullet , \times are from Azzopardi et al.²—gas superficial velocity = 15 m/s.

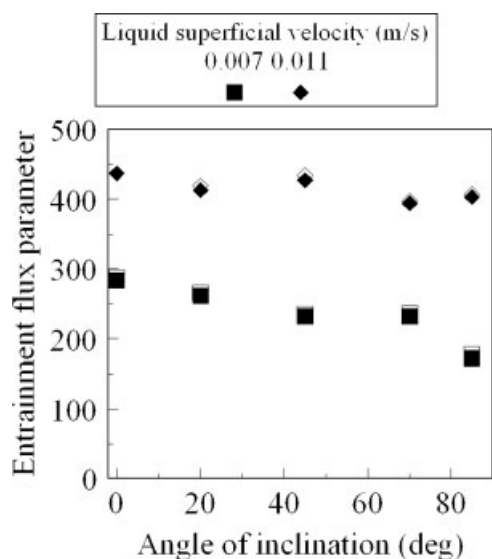


Figure 10. Effect of inclination on entrained flux parameter.

Gas superficial velocity—open symbols = 15 m/s; closed symbols = 21.5 m/s.

quantities of liquid into a film flow whose flow rate was just below the flow rate for formation of waves, they were able to create waves on demand. These experiments, which employed an axial viewing technique, gave very strong proof that drops are only created when there are waves present. Geraci et al.⁴ investigated the effect of inclination on the disturbance wave characteristics. They noticed that in horizontal flow the film interface is covered by large disturbance waves only over the lower half of the pipe, while at the top there are only small amplitude ripples. As the inclination from the horizontal is increased, the amplitude of the disturbance waves decreases, but the fraction of the pipe circumference over which disturbance waves occurs increases. At inclinations close to vertical, disturbance waves are present around the entire section. The interaction between the waves and the gas at the upper half of the pipe balances the lower wave activity at the bottom. Therefore, although there is a greater area of entrainment activity in the 85° inclined pipe it is less intense as the waves are not so big, the total entrained material would be similar to other inclinations.

The wave frequency is another variable that plays an important role in the formation of liquid droplets. In fact, the higher it is the number of the waves passing through the channel in a certain time, the greater the rate of atomization. Geraci et al.⁴ showed that wave frequency is not influenced by inclination at low-liquid superficial velocity (< 0.0317 kg/s). The fact that both friction between waves and gas, and wave frequency are not varying considerably, with inclination is the reason of the trend of the entrained fraction shown in Figure 9. Liquid entrained is not influenced by pipe orientation, and shows a horizontal linear profile at the gas and liquid mass flow rates considered. Higher values of liquid velocity could give more significant variations of liquid entrainment. However, the characteristics of the porous sintered wall unit were not suitable for higher liquid mass flow rates.

The entrained fraction increases slightly with the liquid superficial velocity and decreases slightly with inclination.

Azzopardi et al.² carried out light scattering measurements to determine entrained liquid flow rates in inclined annular gas-liquid flows. Data have been obtained for vertical upward flow and horizontal, as well as inclined flow at 10° intervals in between. Figure 9 illustrates a comparison between these data and those of Azzopardi et al.². It might be expected that a decrease in entrainment, and, hence, of the entrained fraction with increasing inclination would occur, due to the decrease in film flow rate at the bottom as shown in Figures 5–8. However, it is seen that the larger film flow rates occur over a wider part of the pipe circumference as inclination increases. The combination is best seen through the rate of entrainment. Published methods propose that the rate of entrainment is proportional to the film flow rate above a critical film flow rate raised to the power of either 0.736 or 0.925. The critical film flow rate was obtained from the correlation found in Azzopardi,¹³ and can be expressed in terms of the equivalent Reynolds number $Re_{LFC} = 204$. Assuming that this approach from vertical flow can be applied locally around the circumference in inclined flows, and converting local film flow rate to a Reynolds number ($= 4\Gamma/\eta_L$), the entrainment flux can be taken as proportional to $\sum (Re_{LF} - Re_{LFC})^n$. If $Re_{LF} < Re_{LFC}$, the term in brackets is set equal to 0. The resulting values are plotted in Figure 10, where it can be seen that there is a tendency for the flux to diminish with inclination, but only slightly. The rate of entrainment increases with increasing inlet liquid flow rate. It should be noted that with more liquid about a corresponding increase in the rate of deposition is expected. Consequently, the fact that there is little effect of inlet flow rates on the entrained fraction should not be surprising. The trend of entrained flux to decrease with increasing inclination mirrors the behavior of entrained fraction seen in Figure 9.

As no models are available for annular flow in inclined pipes, data for the limiting case of horizontal flow have been compared with prediction the model of Fukano and Ousaka.¹⁸ As can be seen in Figure 11, the predicted film flow rate variation gives a good fit to the experimental results. However, it is noted that the corresponding prediction of circumferential vari-

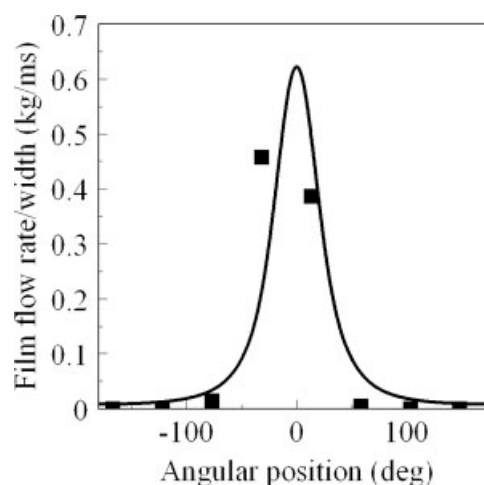


Figure 11. Comparison of predictions of model of Fukano and Ousaka¹⁸ and experimental data.

Gas superficial velocity = 21.5 m/s, liquid superficial velocity = 0.011 m/s. Horizontal.

ation of film thickness shows much poorer agreement with the experimental data as shown by Geraci et al.⁴

Conclusions

The first data for circumferentially resolved film flow rate in pipes inclined at angles from the horizontal to the nearly vertical are presented. These show strong asymmetry when the pipe is horizontal. The asymmetry persists for most inclinations, but decreases systematic with increasing inclination.

At the flow rates studied, the entrained fraction is only very slightly influenced by pipe orientation, and shows little effect of gas and liquid flow rates considered. This is due to the combination of two opposing trends, which are the expected decrease of the entrained fraction with increasing inclination due to the decrease in film thickness at the bottom, and the increase in wave activity as the pipe orientation moves from horizontal toward vertical, which probably results in a liquid entrainment from a large area of the film. The combination of these two trends might balance out and result in the insensitivity of entrained fraction with inclination as reported by this work.

The model of Fukano and Ousaka¹⁸ predicts the circumferential film flow rate distribution for the horizontal case.

Acknowledgments

GG was supported by Shell International Exploration & Production.

Literature Cited

1. Azzopardi BJ, Zaidi SH. The effect of inclination of drop sizes in annular two-phase flow. *4th World Conference on Experimental Heat Transfer, Fluid Mechanics and Thermodynamics Heat Transfer, Fluid Mechanics and Thermodynamics*; Brussels, Belgium; 1997.
2. Azzopardi BJ, Zaidi SH, Jepson DM. Entrained fraction in inclined annular gas-liquid flow. *ASME International Mechanical Engineering Congress and Exposition, Dallas, TX*. 16–21 November 1997.
3. Paz RJ, Shoham O. Film thickness distribution for annular flow in directional wells: horizontal to vertical. *SPE* 28541, 1994:257–272.
4. Geraci G, Azzopardi BJ, van Maanen HRE. Effect of inclination on circumferential film thickness variation in annular gas/liquid flow. *Chem Eng Sci*. accepted.
5. Butterworth D. Air-water annular flow in a horizontal tube. *Progress in Heat and Mass Transfer*. 1972;6:235–251.
6. Butterworth D, Pulling DJ. *Film flow and film thickness measurements for horizontal, annular, air-water flow*. U.K.A.E.A. Report AERE-R 7576 1973.
7. Dallman JC. *Investigation of separated flow model in annular gas-liquid two phase flows*. University of Illinois, Urbana; 1978. PhD Thesis.
8. Laurinat JE. Studies of the effects of pipes size on horizontal annular two-phase flows. University of Illinois, Urbana; 1982. PhD Thesis.
9. Williams LR. Entrainment measurements in a 4-inch horizontal pipe. University of Illinois; Urbana; 1986. MSc Thesis.
10. Paras SV, Karabelas AJ. Droplet entrainment and deposition in horizontal annular flow. *Intl J of Multiphase Flow*. 1991;17:455–468.
11. Ousaka A, Kariyasaki A. Distribution of entrainment flow rate for air-water annular two-phase flow in a horizontal tube. *JSME Intl J. Series II*. 1992;35:354–360.
12. Ribeiro AM, Bott TR, Jepson DM. Drop size and entrainment measurements in horizontal flow. *Two-Phase Flow Modelling and Experimentation*. Celata GP and Shah RK. eds. Edizioni ETS; 1995.
13. Azzopardi BJ. *Gas-liquid flows*. New York: Begell House, Inc; 2006.
14. Taitel Y, Dukler AE. A model for predicting flow regime transitions in horizontal and near-horizontal gas-liquid flow. *AIChE J*. 1976;22:47–55.
15. Taitel Y, Barnea D, Dukler AE. Modelling flow pattern transitions for steady upward gas-liquid flow in vertical tubes. *AIChE J*. 1980;26:345–354.
16. McQuillan KW, Whalley PB. Flow patterns in vertical two-phase flow. *Intl J of Multiphase Flow*. 1985;11:161–176.
17. Azzopardi BJ, Whalley PB. Artificial waves in annular two-phase flow. ASME Winter Annual Meeting, Chicago, Published in *Basic Mechanisms in Two-Phase Flow and Heat-Transfer*. 1980;1–8.
18. Fukano T, Ousaka A. Prediction of the circumferential distribution of the film thickness in horizontal and near-horizontal gas-liquid annular flows. *Intl J of Multiphase Flow*. 1989;15:403–419.

Manuscript received Dec. 6, 2006, and revision received Feb. 20, 2007.